Parametric Modeling of the Current Induced in Linear Conductors

Pradiv Sooriyadevan
Quality Engineering Test Establishment

James Tunaley
London Research and Development Corporation

S. E. Irvine
DRDC – Suffield Research Centre

Defence Research and Development Canada

Scientific Report
DRDC-RDDC-2015-R108
July 2015

Abstract

This report presents computational results of the amplitude of the induced current in a linear conductor and the variation of the amplitude under different external excitation and electromagnetic conditions. For location and avoidance of buried utility cables, the ability to detect linear conductors with a high degree of confidence is important. The report begins with a brief survey of modeling of current induction in conductors and a description of the geometry of the problem, followed by a parametric model analysis using a commercially-available Method-of-Moments solver. The variables addressed in this work are frequency of excitation (50 kHz to 50 MHz), excitation source (plane-wave or dipole), and conductor radius, as well as the conductivity and permittivity of the surrounding soil. The findings herein, as well as those of follow-on studies, will assist in the understanding of electromagnetic scattering from linear conductors and aid in the optimization of devices used to locate them.

Significance to Defence and Security

Reliable sensing of linear conductors is essential, for example, to avoid utilities both in free-space (cable avoidance for aircraft) and underground. Underground applications have become increasingly important since burying utilities has become more favourable than placing them overhead. Sensing buried utilities is not only important in order to reduce the number of accidents associated with excavating, but also to be able to map the continuously expanding hidden infrastructure beneath cities and densely populated areas. The results herein catalogue numerical simulation results which help to understand the physics underlying present methods of locating near-earth linear conductors.

If developed sufficiently with a view to military applications, the results presented here could be applied to detection of command wires associated with improvised explosive devices (IEDs). Such threats are preferred in asymmetric conflicts and must be located in order to be neutralized and mitigate loss of life. Conventional detection technology is not adept at finding such wires and therefore, more research and development is required.

Résumé

Ce rapport présente les résultats computationnels liés à l'amplitude du courant induit dans un conducteur linéaire et à l'écart en amplitude dans des conditions électromagnétiques et d'excitation externe différentes. Pour pouvoir repérer et éviter les câbles enfouis des services publics, il importe d'avoir la capacité de détecter avec très grande certitude les conducteurs linéaires. Le rapport débute par un bref survol de la modélisation de courant induit dans des conducteurs et une description de la géométrie du problème, puis par l'analyse d'un modèle paramétrique au moyen d'un solveur commercial faisant appel à la méthode des moments. Dans ces travaux, on examine les variables suivantes : fréquence de l'excitation (50 kHz à 50 MHz); source de l'excitation (onde plane ou dipôle); rayon des conducteurs; conductivité et permittivité du sol environnant. Les conclusions fournies dans le rapport et celles tirées d'études de suivi aideront à comprendre la diffusion électromagnétique des conducteurs linéaires tout en contribuant à l'optimisation des appareils utilisés pour repérer ceux-ci.

Importance pour la défense et la sécurité

Il est essentiel de pouvoir détecter de manière fiable les conducteurs linéaires, par exemple, pour ne pas nuire aux services publics à la fois dans l'espace libre (afin que les aéronefs puissent éviter les câbles) et dans le sol. Les applications souterraines gagnent en importance de plus en plus, et ce, du fait que l'enfouissement des câbles de services publics est devenu préférable à la pose de câbles aériens. Non seulement est-il important de pouvoir détecter ces câbles enfouis afin de réduire le nombre d'accidents liés aux excavations, mais aussi parce qu'on peut ainsi créer une carte de l'infrastructure cachée qui est par ailleurs en constante expansion sous les villes et les zones densément peuplées. Ce rapport catalogue les résultats obtenus par simulation numérique, ce qui aide à comprendre les principes physiques sous-jacents aux méthodes utilisées actuellement pour repérer les conducteurs linéaires situés près de la surface du sol.

Si les travaux sont élaborés suffisamment en vue d'applications militaires, les résultats présentés ici pourraient être utiles dans la détection de fils de commande d'engins explosifs improvisés (EEI). De telles menaces sont privilégiées dans des conflits asymétriques et doivent être repérées afin d'être neutralisées et réduire ainsi les pertes de vies. La technologie de détection conventionnelle n'étant pas experte pour trouver de tels fils, d'autres travaux de recherche et développement s'avèrent nécessaires.

Table of Contents

This page intentionally left blank.

1 Introduction

The problem of locating buried utilities using electromagnetic means continues to prove difficult given the large variability of conditions associated with such a task. A concrete example is provided in a recent article published by one of the authors [1], where device-specific variables were experimentally studied. Here, a test locating apparatus, comprising a single transmitter and receiver, was constructed and mapped the signal survey profile as the device traversed a single long conductor. In particular, the shape of a signal survey profile had a large variability with orientation of the transmitter as well as the receiver. Indeed the difficulties associated with locating buried conductors were further underscored by the fact that an extremely simple (a single long straight conductor in air) experimental arrangement was implemented. An important issue was the need to determine the absolute amplitude of the current produced within the buried conductor, because this parameter is essentially a measure of the probability of detection (i.e. proportional to scattered field that can be sensed). The current induced in the conductor, and hence its chance of being detected, is influenced by both device-dependent parameters, such as frequency of operation and transmitter-receiver configuration, as well as device-independent parameters associated with the ambient electromagnetic environment. The latter includes soil characteristics and conductor configuration. Investigation into both the device-dependent and independent parameters would undoubtedly aid in optimization of utility locating devices and methods, as well as other applications requiring knowledge of the position of buried linear conductors.

To this end, a modeling approach is adopted to predict the amplitude of current induced in a buried utility by an external electromagnetic source, as well as the variation with parameters such as earth conductivity, permittivity, excitation source, and frequency of excitation. There exists within the scientific literature a large number of studies related to the excitation of currents within long buried conductors. Some examples of analytical approaches include those by Tsubota and Wait [2], Hill [3–4], King [5–7], and Olsen [8–10]. More recent developments include those by Poljak and colleagues [11–12] as well as Naus [13]. Each of these works provided significant advances, yet were limited to a small subset of significant parameters. For example, only certain geometries (e.g. free-space) are considered, or analytical models are limited by their assumptions. As well, the frequencies considered are not relevant to our application. Thus, a comprehensive study of those parameters associated with our specific problem is warranted.

The goal of the present work is to investigate induced current distributions with minimal assumptions or restrictions. As noted, we focus on the induced current as a primary indicator of probability of detection, with the knowledge that any detection device will also bear its own parameters that will influence this probability. That is, the induced current provides a device-independent indication of detection probability. A complete analysis over all ranges of values is unnecessary and narrowed scope is warranted. Selected parameters will be narrowed to ranges that are most relevant to applications involving buried conductor locating [14]. Specifically, the analysis will be limited to the low to high frequency portion of the electromagnetic spectrum (50 kHz – 50 MHz) and finite wires less than 100 m in length. Other parameters will also have limited ranges that are based on the material properties of the conductor in question as well as the surrounding media. The fundamental geometries investigated here include a linear conductor placed in free-space, a uniform infinite dielectric (full-space), and at an air-dielectric interface (half-space). The latter two may have non-zero conductivity, and hence,

are not pure dielectrics. Each of these has respective practical applicability in situations such as cable avoidance systems for aircraft [15–20], borehole-to-borehole studies [21], and buried utility detection [22–23]. In addition to these environmental geometries, additional parameters are investigated and include: excitation by local-dipole or distant-dipole (i.e. plane-wave), frequency of excitation, ground permittivity, ground conductivity, conductor radius and conductor insulating layer, as well as the inter-dependencies between these parameters.

2 Geometry

The geometry of the problem is shown in Figure 1a. In the most general scenario, the linear conductor of length l is considered to be embedded in a dielectric half-space. In all cases, a nominal wire length of 60 m (one free-space wavelength corresponding to f = 5 MHz) is chosen. It is worth noting that the principal resonance of a wire occurs when its length is a half wavelength at the excitation frequency. Additional resonances can occur at multiples of a half wavelength. The upper dielectric is assumed to be air having free-space permittivity ($\varepsilon_a = \varepsilon_0$) and permeability ($\mu_a = \mu_0$) as well as zero conductivity ($\sigma_a = 0$). The lower dielectric, representative of the earth, is non-magnetic and its permittivity (ε_e) and conductivity (σ_e), which are uniform throughout, are characteristic of soil. The linear conductor is located at the interface and is assumed to be 'lying on the surface', with the bottom edge in contact with the lower dielectric.

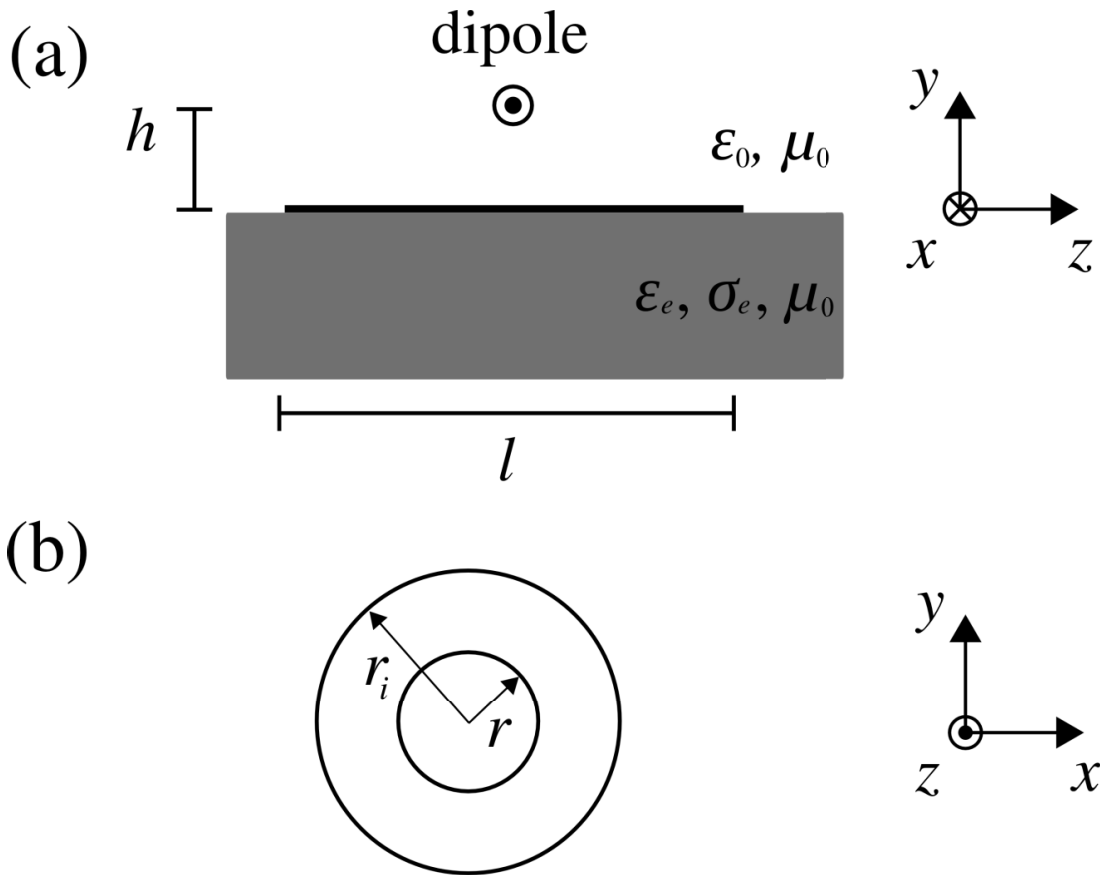

Figure 1: *Physical geometry of electromagnetic scattering from a linear conductor. (a) A wire, of length l, lying on the interface of an air-dielectric interface representing the air-earth boundary. In some cases, a dipole transmitter is located at a vertical height h above the wire. Unless otherwise stated,* $\varepsilon_e = 2.5\varepsilon_0$ *and* $h = 0.1$ *m. In all cases* $\mu_e = \mu_0$*. (b) Cross-section view of the conductor. The conductor itself has the conductivity of copper* ($\sigma_w = 5.7\times10^7$ *S/m) and extends from 0 to a radius of r. The conductor maybe insulated, which would fill the region between r and* r_i*. In cases where the conductor is insulated, the relative permittivity of the insulation is 4.0.*

The location of the wire within the half-space environment is important. For example, the induced current in the wire would change if the wire was embedded in the soil medium instead of the air. Studies are currently underway to investigate this; however, the present manuscript is limited to cases where the wire is lying at the surface with its bottom edge in contact with the earth.

Magnetic dipole and electric dipole excitation sources are considered. It is noted, and discussed in further detail later, that plane-wave excitation can be studied easily in free-space but is more complicated for full- and half-spaces (any attenuation due to propagation would be neglected in software). To address these last two cases, electric dipoles of various orientations are considered (near the end of the analysis) at large distances with their magnitudes appropriately normalized. When the exciter is a local transmitter, a magnetic dipole is positioned at the center of the conductor at a perpendicular height *h*. Given that the origin of the coordinate system (shown in Figure 1) coincides with the center of the wire, the coordinate of the magnetic dipole is

(0, h, 0). Unless otherwise stated, h = 0.1 m. In some cases that follow, it is considered that the linear conductor may be located in free space or in an infinite non-magnetic dielectric material, i.e. full-space. In an infinite dielectric, the dipole and linear conductor are embedded in the dielectric, in which the permittivity and conductivity are uniform.

A cross-sectional view of the conductor is illustrated in Figure 1b. The center cylinder of radius r is solid metal having high conductivity σ_w and free-space permeability μ_0. The solid center can be surrounded by an insulating jacket with a permittivity ε_i, free-space permeability μ_0, and zero conductivity. The insulator is a cylindrical shell filling the region space between r and r_i along the length of the wire. In most cases the radius of the linear conductor is chosen to represent a single wire with r = 0.5 mm. In cases where the wire is insulated, r_i = 1.5 mm and $\varepsilon_i = 4.0\varepsilon_0$. The material parameters of the wire conductor are chosen to represent copper: $\sigma_w = 5.7 \times 10^7$ S/m, $\mu_w = \mu_0$. Unless otherwise stated, the permittivity of the earth is $\varepsilon_e = 2.5\varepsilon_0$. Again, it is assumed that the bottom edge of the conductor, whether it is bare or insulated, is in contact with the lower dielectric.

3 Modeling Considerations

Practically, many survey and locating devices transmit at a single frequency and therefore the analysis presented here will be also be restricted to a single frequency (although this parameter itself will be varied). It is also important to consider that the linear conductor has a large aspect ratio ($l/r > 10^5$). Therefore the natural choice for performing numerical computations of the current induced in the wire is through the Method of Moments (MoMs) [24]. This allows for full-wave solution with limited computational overhead.

The software that has been chosen to perform the calculations is FEKO (EM Software & Systems, Stellenbosch, South Africa), which contains a MoMs solver. Linear basis functions are used to model the wire, and the insulating jacket is accounted for using the Volume Equivalence Principle [25]. The latter shortens computation time substantially and its validity was verified against standard MoMs using FEKO (which yielded identical results). The particular Green's function selected in FEKO is a Planar Multilayer Substrate. In the cases presented here, there are two layers: the air and the earth. Selected FEKO results are compared with an analytical model in Annex A to provide a measure of confidence in the analysis.

In order to obtain meaningful magnitudes of the current amplitude, an appropriate source power must be chosen. In the case of local excitation, a magnetic dipole is used. Its axis is oriented horizontally and perpendicular to the wire. The magnitude of the dipole moment is chosen to represent a small portable transmitter having a power on the order of 1 W; this equates to a magnetic dipole amplitude of 0.003 $A \cdot m^2$. For plane-wave excitation in free-space, the magnitude of the applied electric field is 1 V/m. This will be discussed near the end of the report. Both local and plane-waves are considered as the exact distribution of the excitation field will influence the profile of the induced current on the wire.

4 Numerical Analysis and Results

4.1 Free-Space

We first consider the effect of frequency on the induced currents within the wire. Shown in Figure 2 are several plots of the current distribution in a wire located in free-space. The frequency takes on the values of f = 50 kHz, 500 kHz, 5 MHz, and 50 MHz. Several panels are shown for various combinations of bare or insulated conductors and dipole or plane-wave sources.

Figure 2a shows the current in the bare wire induced by the magnetic dipole. The current falls off linearly to zero at the ends of the wire as illustrated for the bare wire with magnetic dipole excitation at 50 and 500 kHz. Figure 2e and 2f show the same response on a linear scale; the response is approximately triangular. As the frequency increases from 50 kHz, the current increases. Part of this increase is due to the fact that the electric field amplitude of a dipole is linearly proportional to f [26]. At frequencies of 5 MHz and 50 MHz, the current is spatially modulated. The current distribution at 5 MHz resembles a plot for the current in a centre-fed full wavelength dipole in King et al. 2002 [27]. At 50 MHz, the wire is ~10 wavelengths in length and there are 20 peaks corresponding to resonances over approximately 20 half wavelengths.

When the bare wire is excited using a plane wave instead of a magnetic dipole, the method of excitation introduces important differences as shown in Figure 2b. At 5 MHz there is only one peak rather than two. At 50 MHz, there are 10 peaks rather than 20. These features are due to a fortuitous suppression of intervening spatial troughs as a result of resonance on the wire together with the method of excitation. The responses also change slightly at the lower frequencies.

The current in the insulated wire excited by a magnetic dipole is shown in Figure 2c. The plots are similar to those in Figure 2a except at 50 MHz where there are now 21 peaks because of the effect of the insulation in reducing the magnitude of the propagation speed along the wire. At the lower frequencies there only minor differences due to insulation. Except at 50 MHz, insulation has a minor effect on both the current response along the wire and its amplitude. In this last case, the insulation (with a relative permittivity of 4) increases the coupling between the exciter and the wire.

When the insulated wire is excited by a plane wave, the results of which are shown in Figure 2d, the response at the two lower frequencies is not substantially different from that of a bare wire. At 5 MHz, there is one peak, as for the bare wire, but the insulation has reduced the magnitude of the propagation speed so that the wire length is now somewhat greater than a wavelength; the response at its ends reflects this fact. At 50 MHz, the response is greater than for the bare wire and intervening troughs are no longer completely suppressed because the wire length is no longer close to an exact multiple of the wavelength.

As noted by Hill [3], the current distribution is weakly dependent on the radius of the inner conductor in both shape and amplitude. This has been verified for nearly all of the cases described so far. Exceptions are illustrated by Figure 3 for an insulated wire at a frequency of 50 MHz in free space. The internal impedance of the wire is a function of its radius as are the fields in the insulation and the air. Changes in these affect the propagation constant of the current on the wire.

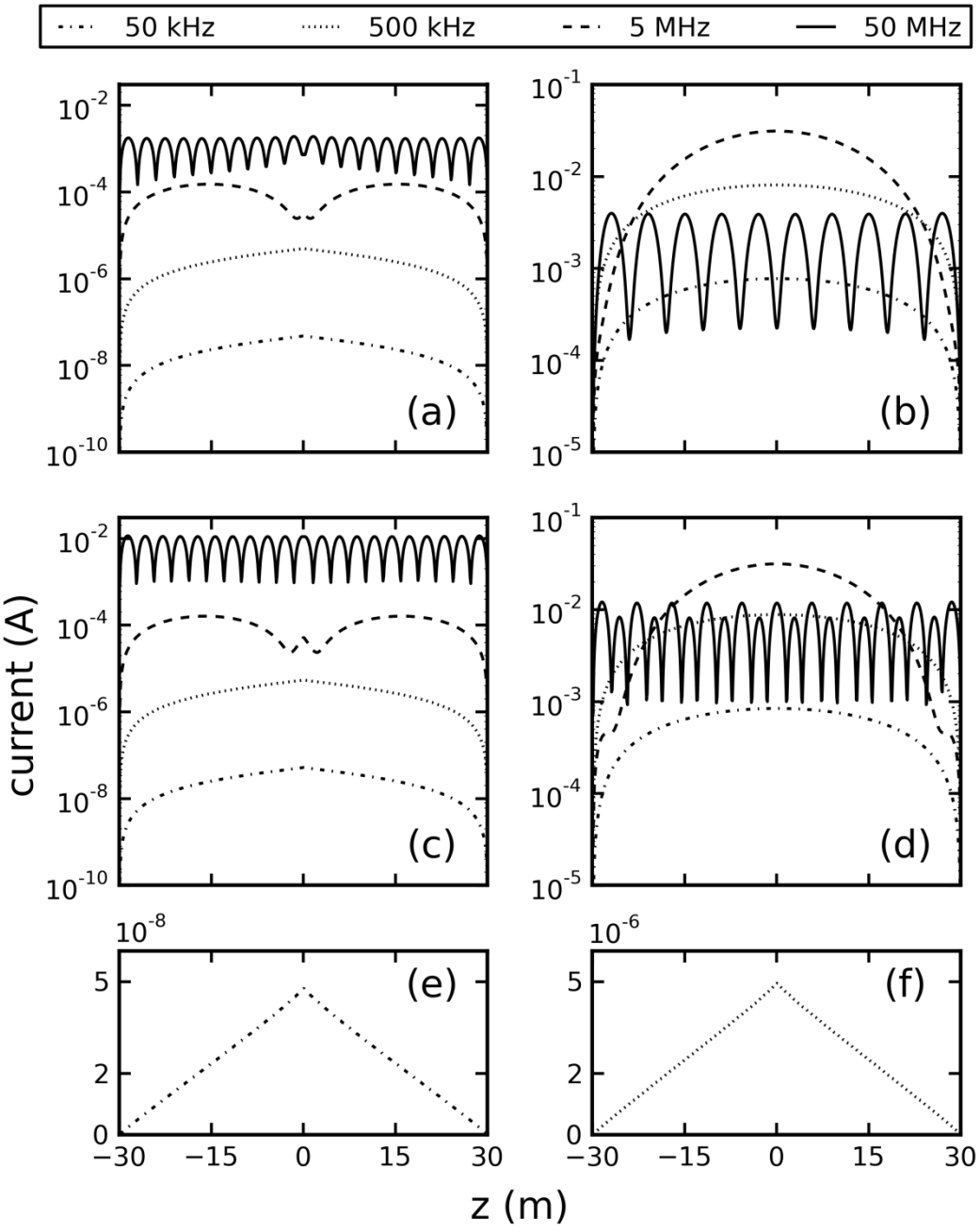

Figure 2: *Illustration of the effect of frequency on excitation of current in free space for four frequency values. The various panels represent different combinations of bare or insulated wire and dipole or plane-wave excitation sources. They are (a) bare and dipole, (b) bare and plane-wave, (c) insulated and dipole, and (d) insulated and plane-wave. In cases that implemented a dipole source, h = 0.1 m. Panels (e) and (f) correspond to the respective 50 kHz and 500 kHz curves in (a) but are plotted on linear scales.*

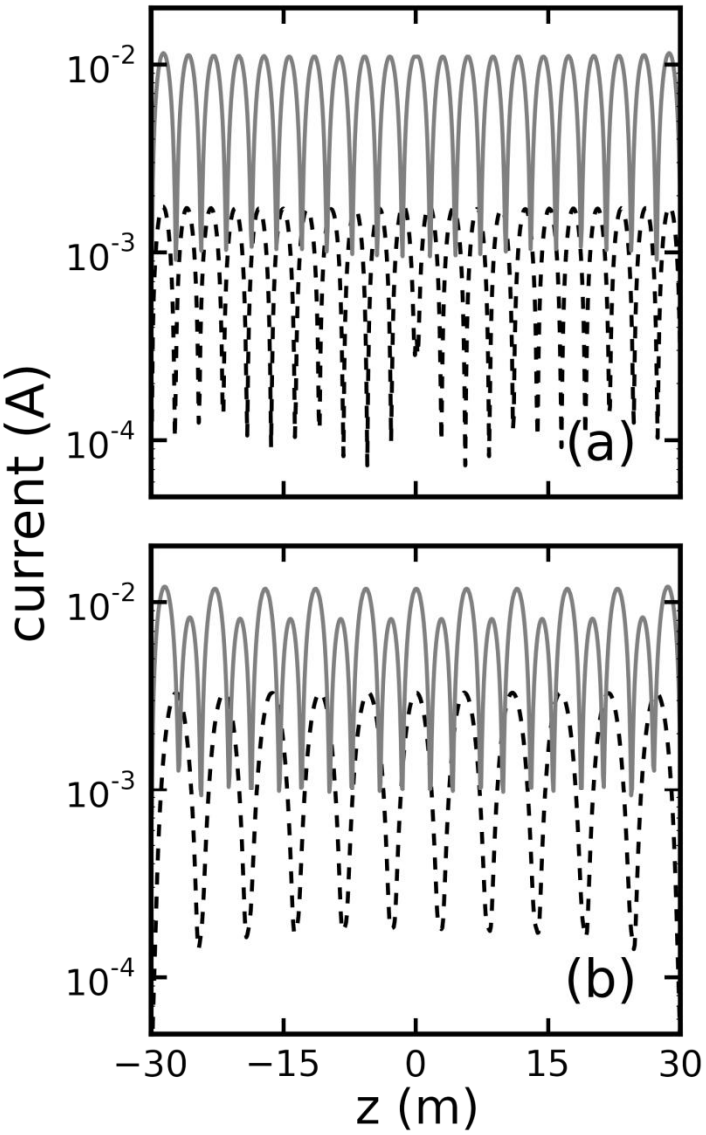

Figure 3: *The effect of changing the conductor radius r in the case of an insulated conductor and f = 50 MHz. The insulator thickness was held fixed and therefore, the quantity $r_i - r$ was held constant at 1 mm. Two values for wire radii have been used and are 0.5 mm (solid gray) and 1.0 mm (dashed black) for both a (a) dipole and a (b) plane-wave source.*

The phase of the propagating wave and the overall amount of interference are altered. Near resonance, only a small change in the wave-vector is required to significantly modify the current profile. This is evidently the case for an insulated wire excited at 50 MHz, but the effect becomes negligible at lower frequencies.

4.2 Dielectric Full and Half-Spaces

The next portion of the analysis describes the effects of the media surrounding the conductor; these correspond to free-, full- and half-spaces. In an effort to keep the number of solutions tractable, the frequency will be limited to values of 500 kHz or 5 MHz for the remainder of the analysis. Furthermore, only the magnetic dipole source will be considered for the next portion of the investigation. Figure 4a illustrates the current distribution in an insulated wire for the two frequencies and the three distinct dielectric spaces. It is observed that the distributions in the case of 500 kHz (well below resonance in all cases) are very similar; they correspond to responses that are approximately triangular as in free space. The amplitude of the current in these cases depends on the local effective dielectric constant. The larger the effective dielectric constant, the better is the coupling between the dipole and the wire, which results in larger currents.

Conversely, data shown for 5 MHz indicate that the type of dielectric space can greatly influence the distribution shape at higher frequencies. The higher frequency leads to larger current amplitudes (again magnetic dipole excitation implies that the response includes a frequency factor). Thus, for locating applications, larger frequencies may be more suitable to increase probability of detection. Other applications may require, for example, a more uniform probability of detection along the length of the wire, and in these cases, a lower frequency of excitation may be more applicable.

Shown in Figure 4b is the variation of current amplitude in the conductor with dipole height above ground for the half-space case. The conductor is located at the interface of a dielectric half-space while h is varied from 0.1 to 1.0 m. As expected, the amplitude decreases as the dipole exciter is moved further away from the wire. It is important to note that while the amplitude drops off by more than an order of magnitude, the shapes of the current distribution do not change significantly over this range of h values. If the dipole is moved very far away compared to the wavelength, the distribution approaches that which is produced by a plane-wave source (not shown). The trend is similar for other choices of frequency and dielectric values. Also shown in Figures 4c-e are the variations of current amplitude at the center of the wire with the dipole height above the wire, h. In all cases, a nearly inversely proportional relationship is observed.

Aside from the particular dielectric space configuration (free, full, or half), the contribution from the earth conductivity can also dramatically affect the current induced within the conductor. To explore this we first consider the full-space environment, in which the conductor is surrounded by an infinite dielectric. The full-space scenario, from the standpoint of practical relevance, applies to borehole-to-borehole studies. Shown in Figure 5 are numerous current distributions corresponding to various values of realistic earth conductivity σ ranging from 0 S/m to 1 S/m, albeit the upper limit would be consistent with an extremely mineralized soil or sea water [28–31]. Moreover, the conductor is either bare or insulated and the frequency of excitation is 500 kHz or 5 MHz.

For the data in Figure 5, magnetic dipole excitation has been used (a plane-wave-like scenario will be discussed later). Immediately it is observed that the current distribution can change greatly depending on the frequency, dielectric material and the presence of an insulating layer, which are all important variables. Figure 5a shows the bare wire response at 500 kHz. When the conductivity of the dielectric is small, the response resembles that for free space and on a linear scale the response is approximately triangular. As the conductivity increases the waves become

strongly damped as they propagate away from the excitation. However, the coupling between the exciter and the wire tends to increase and this produces larger amplitudes close to the exciter. The reason for the larger coupling is the increase of the propagation constant (i.e. decrease in effective wavelength) of the impinging wave in the host medium that is due to the increase in conductivity.

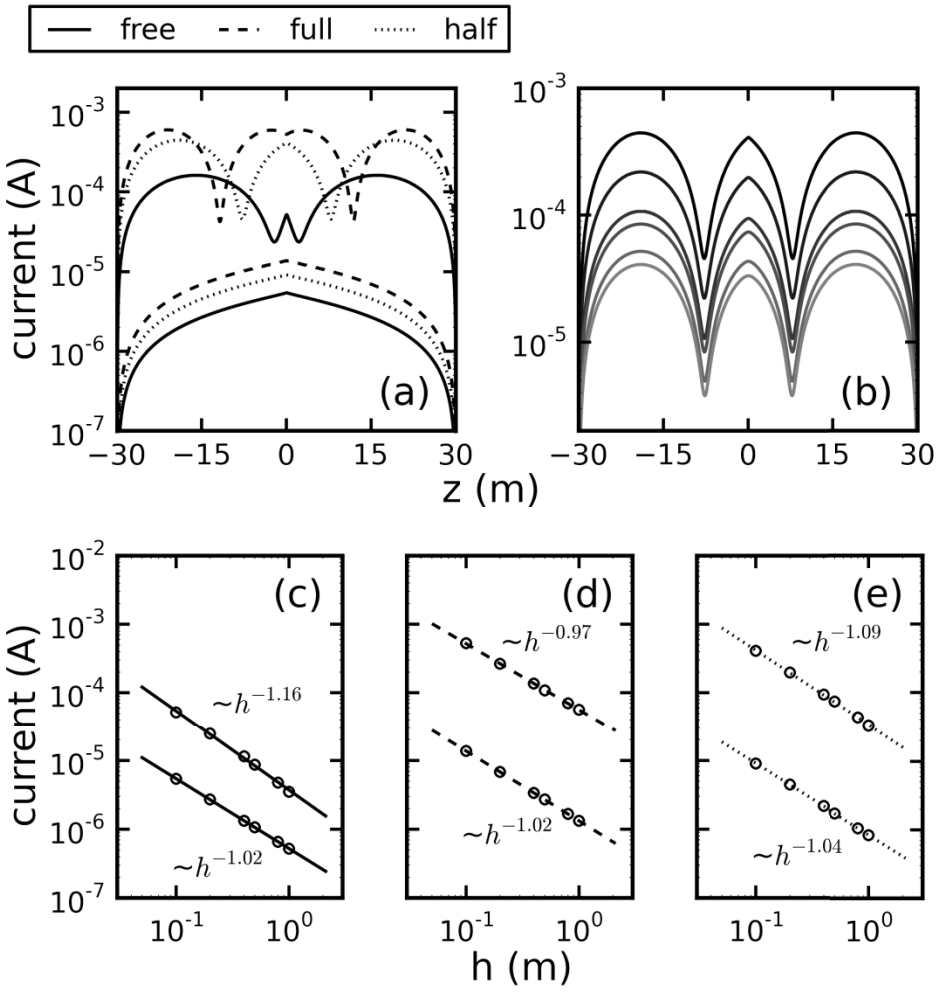

Figure 4: *(a) Illustration of the effect of local dielectric configuration on the current distribution in an insulated wire. Three cases were chosen, all having $\sigma_e = 0$, and correspond to free-space (solid line), a uniformly filled full-space having $\varepsilon_e = 2.5\varepsilon_0$ (dashed line), and a half-space (dotted line) filled with a similar dielectric representing soil. For the latter case, the conductor lies on the interface of the vacuum dielectric boundary (which represents the earth). The lower curves are for f = 500 kHz while the uppers ones are for f = 5 MHz. (b) Variation of the current distribution with dipole height above the wire for the case of 5 MHz and the dielectric half space. Several plots are shown and progress from smallest height (black) to largest height (light gray) with values of h = 0.1, 0.2, 0.4, 0.5, 0.8, and 1.0 m. Over this range, the amplitude of the induced current is reduced by nearly an order of magnitude. The trend is similar for other choices of frequency and dielectric values. The final three panels summarize the results, amplitude versus h, for all three different spaces: (c) free, (d) full, and (e) half.*

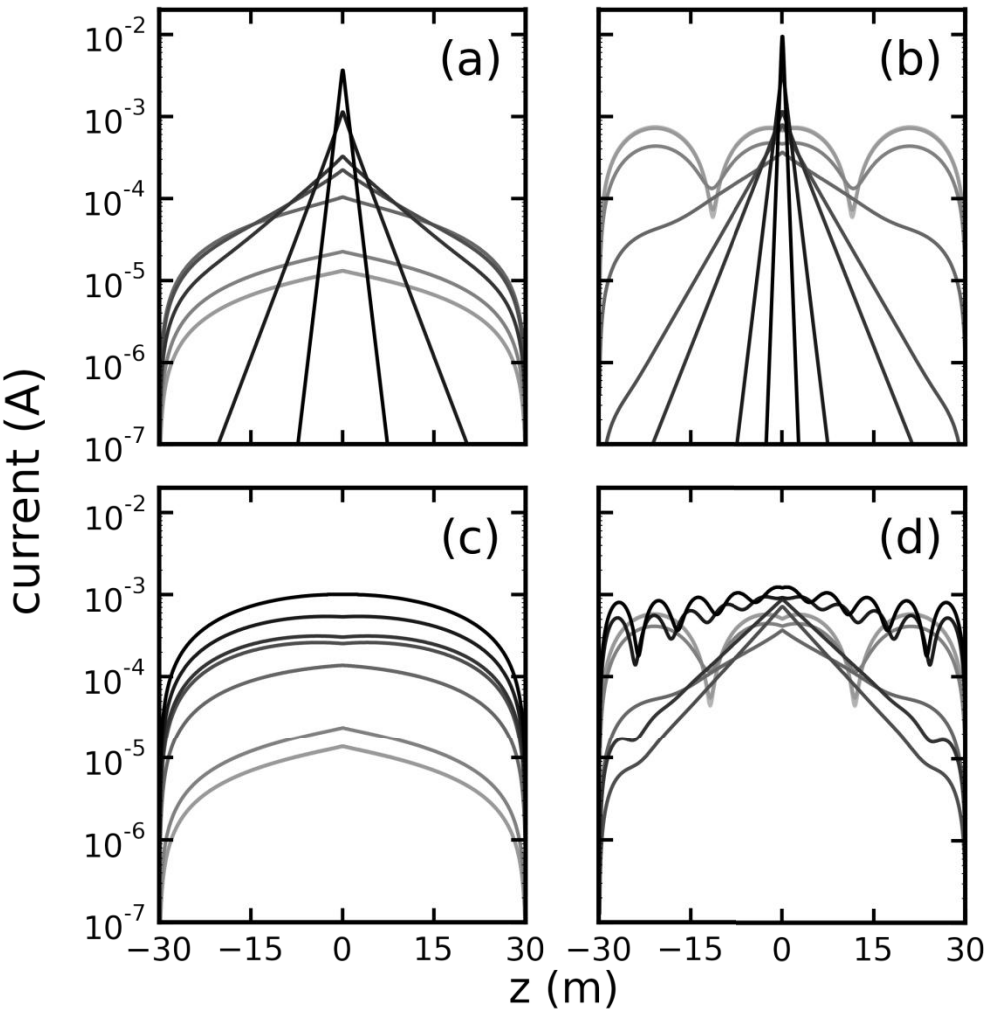

Figure 5: *The effect of ground conductivity on induced current in a full-space environment. The relative permittivity of the ground is held at 2.5 while σ_e is varied from 0 (light gray) to 1 S/m (black). The particular values of the conductivity are σ_e =0, 1 × 10^{-6}, 1 × 10^{-5}, 1 × 10^{-4}, 1 × 10^{-3}, 5 × 10^{-3}, 1 × 10^{-2}, 1 × 10^{-1}, and 1.0 S/m. Analysis was performed for various combinations of frequency and wire coating, which are (a) bare and 500 kHz, (b) bare and 5 MHz, (c) insulated and 500 kHz, and (d) insulated and 5 MHz. In panels (a)-(d), the curves for σ_e = 0, 1 × 10^{-6} S/m, 1 × 10^{-5} S/m are overlapping.*

At 5 MHz, the bare wire response is depicted in Figure 5b. When the conductivity is low, damping is small and the permittivity of the dielectric slows the waves on the wire; there are 3 peaks appropriate to a relative permittivity of 2.5; peaks occur at intervals of a half wavelength. As the conductivity rises, the peaks disappear and again the waves become strongly damped.

Figure 5c shows the responses for an insulated wire at 500 kHz. The insulation is very effective in reducing the attenuation associated with losses in the medium. As a result, the current increases

with conductivity because of increased coupling to the exciter (larger σ_e results in a shorter effective wavelength).

At 5 MHz and when the conductivity is small, insulation makes little difference to the response, as shown in Figure 5d. As the conductivity rises, it dominates the dielectric properties near the wire and causes the waves to be damped. With further increase in conductivity, the dielectric outside the insulating sheath acts like a coaxial outer conductor and the wave propagation becomes heavily influenced by the properties of the insulation, which has a relative permittivity of 4. If this outer conductor were perfectly conducting, the wire would be two wavelengths long, which would result in 4 peaks. However, there are 9 peaks and this is due to a further reduction of the wave propagation speed associated with the finite conductivity of the earth.

For completeness, the effect of ground permittivity is also considered while holding the conductivity fixed at $\sigma_e = 0$. Figure 6 shows several current distributions for relative permittivities ranging from 1 to 100. Panel (a) shows the results for a bare wire excited by a magnetic dipole at 500 kHz. Increasing the permittivity slows the waves by a factor equal to its square root. Therefore, when the relative permittivity is 100, the wavelength is equal to the length of the wire and the shape of the response is practically identical to that in Figure 2a; it corresponds to a full-wave resonance. Otherwise on a linear scale the responses are approximately triangular.

Similarly Figure 6b shows the responses at 5 MHz. These show the expected number of peaks according to the relative permittivity. When the wire is insulated, the insulation changes the effective permittivity near the wire and Figure 6c demonstrates that, when the relative permittivity of the ground is 100, the wavelength is no longer a multiple of a half wavelength. The results in Figure 6d are consistent with the concept of the domination of the dielectric properties near the wire by the insulating sheath, especially when the relative permittivity of the ground is large.

4.3 Comparisons of Full- and Half-Space Current Profiles

Arguably, the most interesting scenario to consider is the half-space since many applications involve conductors near the surface of the earth. The wire is considered to be lying on the ground and its outermost edge, whether insulated or bare, is in contact with the ground or lower dielectric space. To begin it is considered that currents are induced by a local magnetic dipole that is elevated above the wire by the same amount as previously, i.e. h = 0.1 m. Thus, the set of simulations shown in Figure 5 is essentially repeated, but now with the half-space geometry.

First consider the bare wire half-space responses shown in Figures 7a and 7b, which respectively illustrate current distributions for f =500 kHz and f =5 MHz. There is a clear dependence on the conductivity but it is not as pronounced as for the full-space. In the case of f =500 kHz, as the conductivity is increased the amplitudes of the current distributions increase as well, but saturate much earlier than the case of the full-space. For the higher frequency plots in (b), it is observed that the conductivity affects the profiles but not to the same degree as when the wire is located in a full-space (Figure 5). It is noted that while the current distributions in the case of the half-space indicate variations of spatial modulation with σ_e, their amplitudes are more uniform. That is, they do not show as much decay as the ends of the wire are approached, which clearly differs from the full-space case in Figure 5. A similar statement can be made for the insulated wires embedded in

a half-space, the results of which are shown in Figures 7c and 7d. The principle result of this particular analysis is that the addition of an air layer above the wire has a moderating effect when the conductivity is allowed to vary.

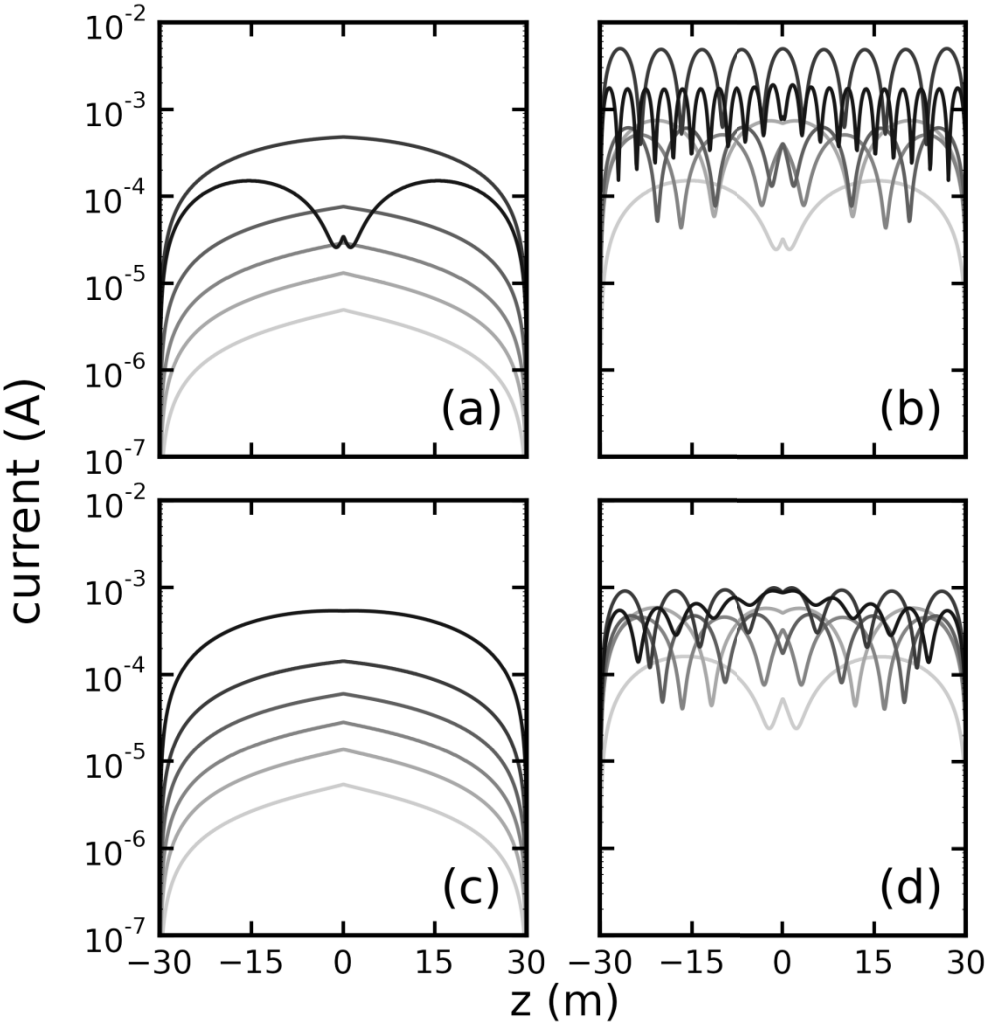

Figure 6: *The effect of ground permittivity on induced current in a full-space environment. The conductivity of the ground is held at σ_e = 0 while the relative permittivity is varied from 1 (light gray) to 100 (black). The particular values of ε_e are 1, 2.5, 5, 10, 20, and 100. Analysis was performed for various combinations of frequency and wire coating, which are (a) bare and 500 kHz, (b) bare and 5 MHz, (c) insulated and 500 kHz, and (d) insulated and 5 MHz.*

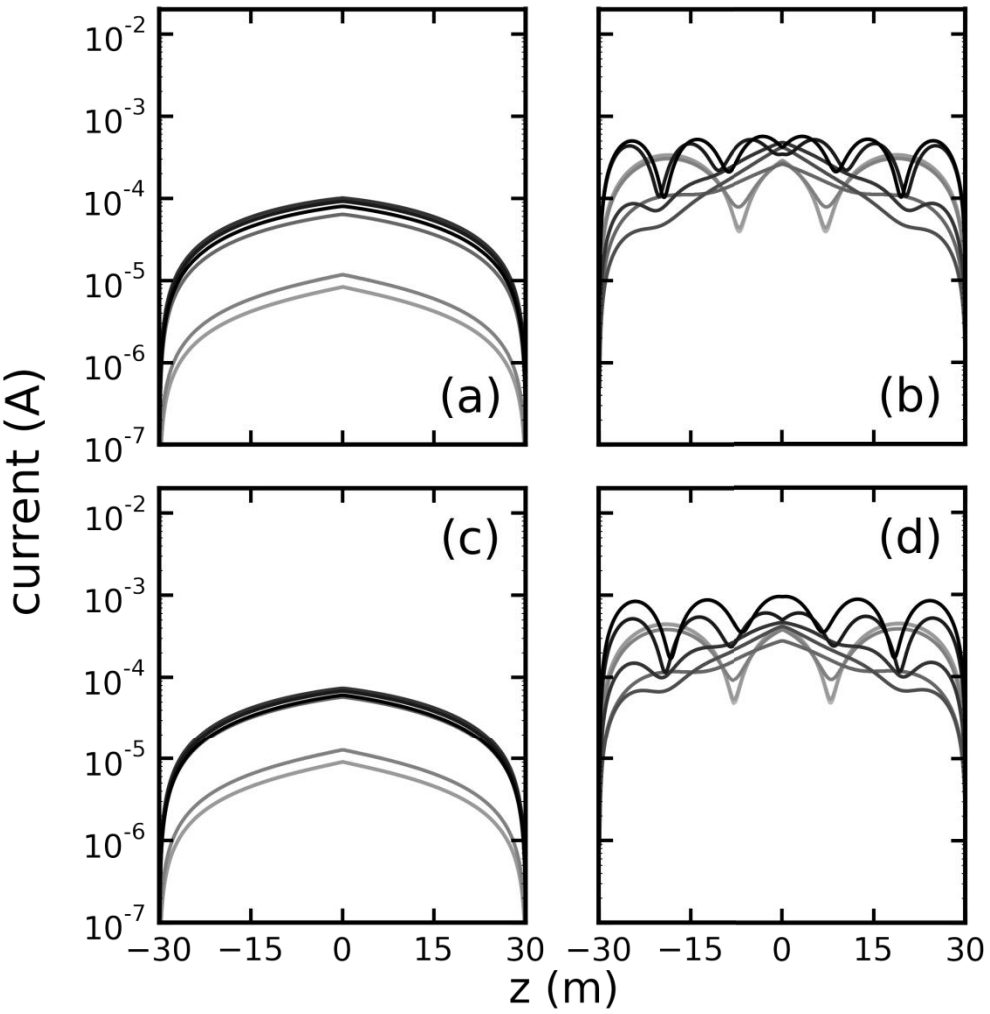

Figure 7: *The effect of ground conductivity on induced current in a half-space environment. The relative permittivity of the ground is held at 2.5 while σ_e is varied from 0 (light gray) to 1 S/m (black). The particular values of conductivity are σ_e = 0, 1 × 10^{-6}, 1 × 10^{-5}, 1 × 10^{-4}, 1 × 10^{-3}, 5 × 10^{-3}, 1 × 10^{-2}, 1 × 10^{-1}, and 1.0 S/m. Analysis was performed for various combinations of frequency and wire coating, which are (a) bare and 500 kHz, (b) bare and 5 MHz, (c) insulated and 500 kHz, and (d) insulated and 5 MHz. In panels (a)-(d), the curves for σ_e = 0, 1 × 10^{-6} S/m, 1 × 10^{-5} S/m are overlapping.*

We also consider the variation of permittivity, while keeping the conductivity constant, in the half-space geometry. Results are shown in Figure 8 for a relative permittivity ranging from 1 to 100 and σ_e = 0. The overall results of increasing the relative permittivity are similar to those presented in Figure 6. Again, going from a full-space to half-space geometry, it is noted that the air layer above the dielectric moderates changes in permittivity as well as conductivity.

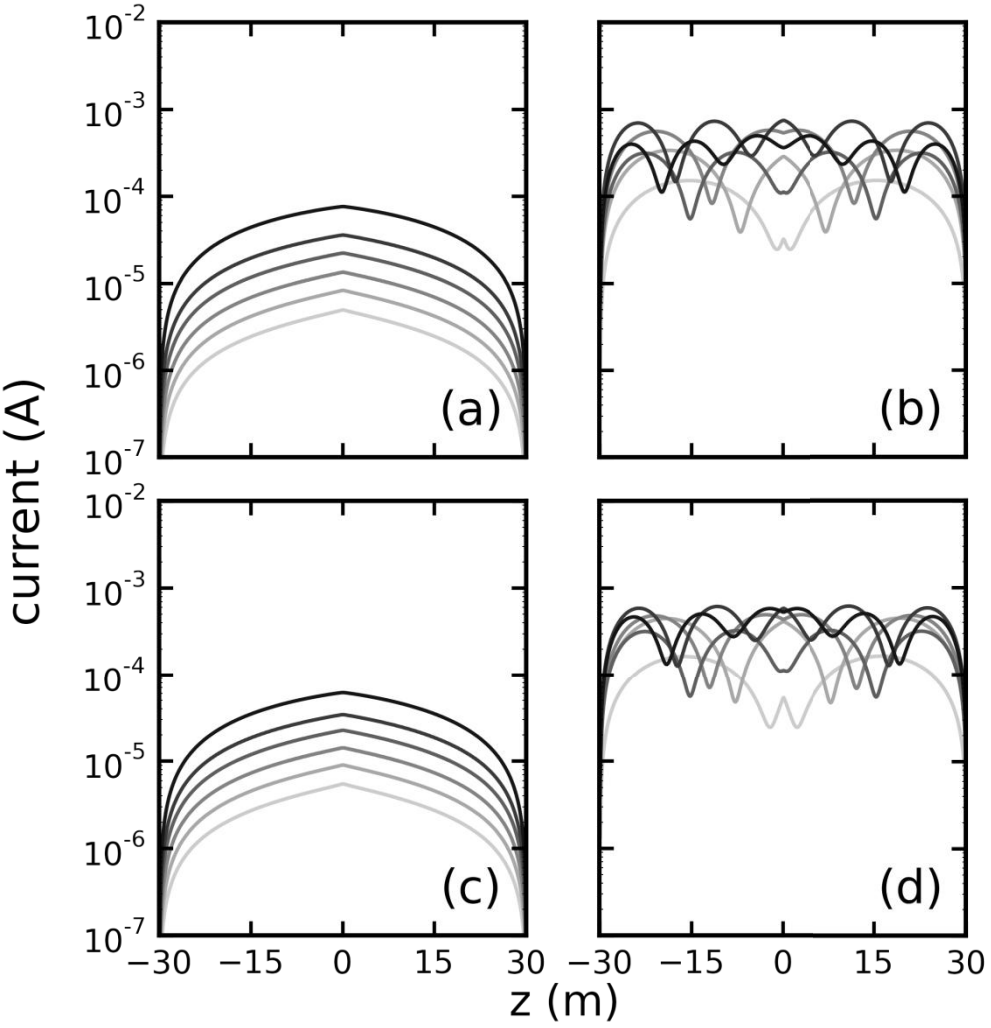

Figure 8: *The effect of ground permittivity on induced current in a half-space environment. The conductivity of the ground is held at $\sigma_e = 0$ while the relative permittivity is varied from 1 (light gray) to 100 (black). The particular values of ε_e are 1, 2.5, 5, 10, 20, and 100. Analysis was performed for various combinations of frequency and wire coating, which are (a) bare and 500 kHz, (b) bare and 5 MHz, (c) insulated and 500 kHz, and (d) insulated and 5 MHz.*

4.4 Distant Transmitter

Thus far, in the full and half-space configurations, only magnetic dipoles sources are considered. We also include an analysis of distant or plane-wave electric dipole sources. In the beginning of the analysis in this paper, in which free space plane-waves are considered (Figure 2), it is sufficient to simply assume a uniform electric field along the length of the wire. Indeed, in MoMs calculations, the assumption of a plane-wave allows a simplification of the integrals involved. Namely, the electric field is set to a particular uniform constant value and can be moved outside the integral operator in the field equations [32].

Meaningful comparisons for plane-wave excitation can only be made if account is taken of propagation losses due to conductive ground. Otherwise changes in the conductivity of the ground would only affect the coupling of the excitation to the conductor. To achieve an approximation to plane-wave excitation, the electric dipole should be placed as far as possible from the conductor. However, a limitation is placed by the FEKO software program [33]; a maximum standoff distance of 10 wavelengths is permitted. Therefore a comparison basis involves a horizontally polarized electric dipole placed in free space at a distance of 6 km at 500 kHz and 600 m at 5 MHz. This provides a relation between the electric dipole moment of the exciter and the field strength at the conductor. Comparisons are made by using the same dipole moment, located close to the ground, for all dielectric configurations. The moment is chosen so that the results in Figure 2 would be reproduced for free-space. It is important to note that the remaining analysis is restricted to insulated wires.

Several dipole-wire orientations are also considered partly because vertical electric dipoles are more common in practice. The results are depicted in Figure 9. It is clear that each parameter significantly affects the current distribution. Panels (a) and (b) contain results that are closest, in terms of parameters, to the distant-dipole full-space results shown in Figure 10. In Figures 9a and 9b, a horizontal electric dipole is used to excite currents in a wire oriented along the same direction as the dipole, i.e. both are along the z axis. This represents a strong coupling case. The air layer of the half space drastically alters the current distributions relative to Figure 10 both in terms of amplitude and shape. Increasing soil conductivity does not reduce the amplitude as much for the half-space as the full-space. Again this clearly indicates that the air layer has a moderating effect (compare the results in Figures 9b and 10b for example).

Next, the dipole orientation is changed to vertical, while the wire orientation remains fixed, i.e. the dipole vector is along y and the wire is along z. The results are shown in panels 9c and 9d. In such a situation, the dipole and wire are nominally cross polarized and in free space there would be no excitation. However, in a half space the electric field from a vertical antenna becomes elliptically polarized and exhibits a significant horizontal polarized electric field component in the direction of propagation [27]. If the wave front is slightly curved, this component can excite currents in the wire; order of magnitude estimates suggest that this mechanism is responsible for the responses and is consistent with the large null at the center of the wire.

The final set of orientations is with the dipole along y and the wire along x (end-fire configuration). The results are shown in panels (e) and (f) and again the horizontal component of the electric field in the direction of propagation is responsible for the excitations. It is interesting to note that the lower frequency, f =500 kHz, curves retain their symmetry, which is lost at the higher frequency, f =5 MHz. This is a result of the relative size of the wavelength compared to the wire. For the lower frequency, the wavelength is much longer than the wire, and thus, the phase of the current changes slowly as it alternates back and forth along the wire (the wire length is only one-tenth of the free-space wavelength). The dynamics are much more complex at f =5 MHz, as there are now pronounced interference effects on the wire (forward and reverse propagating modes).

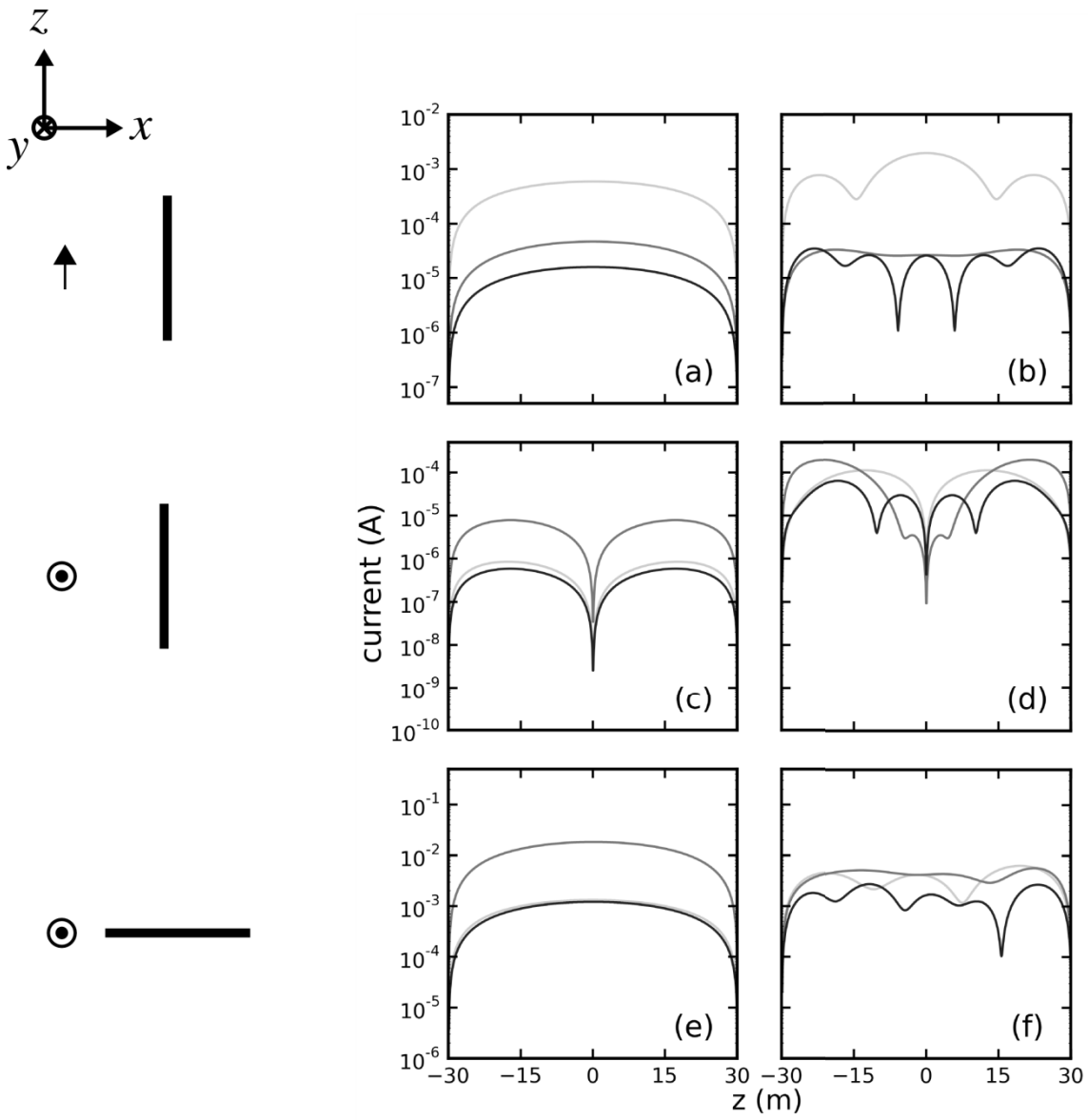

Figure 9: *Illustration of a half-space quasi-plane-wave scenario, in which an electric dipole was placed at a distance of 10 wavelengths away from an insulated wire. The current distributions shown here are for 3 values of conductivity σ_e = 0 (light gray), 5 × 10^{-3} S/m (gray), and 1 S/m (black). The simulations were performed for two frequencies (a,c,e) 500 kHz and (b,d,f) 5 MHz. Several dipole-wire orientations are considered and are illustrated in the figure.*

In all low-frequency cases in Figure 9, it is noted that an increase in conductivity leads to a decrease in current amplitude: an effect which results from attenuation during propagation in the surrounding media, albeit at a much lower rate than the full-space scenario. The situation appears to be much more complicated, however, for the higher frequencies. For some orientations (e.g. panel (b)), there are similar trends. However, for the other orientations, it appears that the effect is reduced. For example, in panel (f), only a small reduction is noted, but the shape of the

distribution is altered. In this case, the increase in conductivity may alter phase-matching conditions. That is, while conductivity may increase attenuation rate and reduce current amplitude, the current wave on the wire may be better matched to the incoming wavelength and result in better coupling.

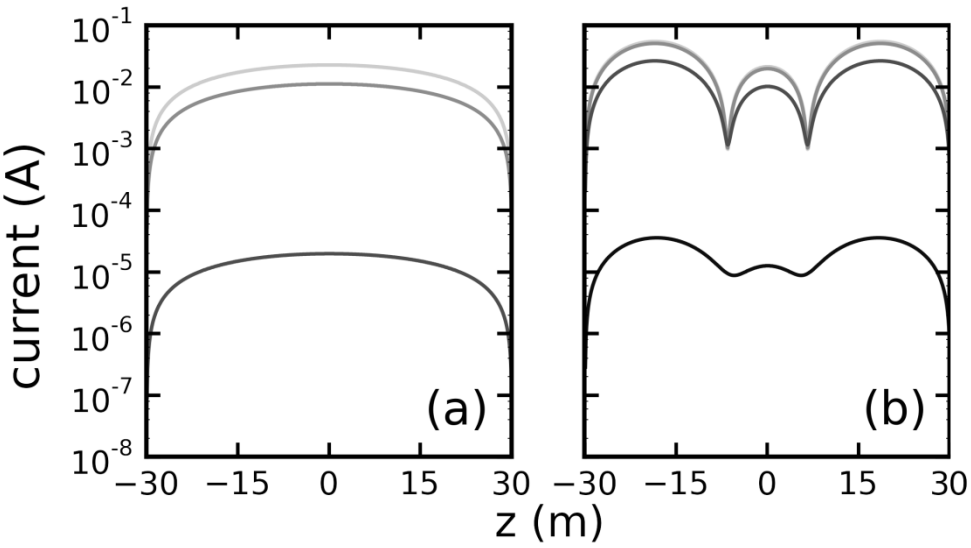

Figure 10: *Illustration of a full-space quasi-plane-wave scenario, in which an electric dipole was placed at a distance of 10 wavelengths away from an insulated wire with the dipole parallel to the wire. The simulations were performed for two frequencies (a) 500 kHz and (b) 5 MHz. The current distributions shown here are for various values of conductivity* σ_e *ranging from 0 (light gray) to* 1×10^{-4} *S/m (black). The particular values are 0,* 1×10^{-6}*,* 1×10^{-5}*,* 1×10^{-4} *S/m. Note that the maximum conductivity used for these results is four orders of magnitude lower than the maximum value used in Figure 9. It is noted that the current distribution corresponding to* $\sigma_e = 1 \times 10^{-4}$ *S/m is not shown in (a) since its amplitude is too low. In panel (b), the curves for* $\sigma_e = 0$ *and* $\sigma_e = 1 \times 10^{-6}$ *S/m are overlapping.*

The full-space quasi-plane-wave excitation of Figure 10 is now reconsidered in detail. Attenuation in the ground is expected to damp the incoming wave and, though such a scenario is possibly of less practical importance, it is included here for completeness. Shown are several current distributions for insulated wires at frequencies of 500 kHz and 5 MHz, as well as several values of soil conductivity σ_e. For the case of $\sigma_e = 0$ and $f = 500$ kHz (panel (a)), it is observed that a larger current amplitude is obtained compared to its free-space counterpart shown in Figure 2d; this is due to better coupling (i.e. reduced wavelength of the incident radiation by a factor equal to the square root of the relative permittivity or the refractive index of the ground ($\sqrt{2.5}$). Immediately, it is also clear that attenuation in the full-space plays a very large role, as expected. Over a propagation distance of 10 wavelengths, only moderate values of σ_e diminish the current values to negligible amounts. For cases shown previously, in which the transmitter was a local magnetic dipole, changes in the local conductivity resulted in large changes in the shapes of the current distributions, with small or moderate changes in their amplitudes (resulting principally from near-field coupling). Evidently, this is not the case in the distant-dipole full-space geometry, as attenuation during propagation plays the dominant role. Referring to panel (a) with

f = 500 kHz, with an increase of σ_e from 0 to 1×10^{-5} S/m, the current amplitude is reduced by 3 orders of magnitude. Nearly identical results occur for the higher frequency case (f =5 MHz), shown in panel (b). It is noted, however, that a similar decrease in amplitude occurs for σ_e ranging up to 1×10^{-4} S/m. This is due to the fact that the dipole distance of 10 wavelengths at 5 MHz is 10 times closer than in the case of 500 kHz.

5 Conclusion

We have presented numerical investigations of the currents induced in a linear conductor lying on the surface of the earth. Several geometries have been reviewed, which include a uniformly-filled dielectric space, free space, and a dielectric half-space. Within this analysis, the variation with type and location of the transmitter has been discussed. Finally, the effects of the local dielectric parameters, such as permittivity and conductivity, have been quantified. Evidently the entire range of values for each parameter cannot be explored in a single study, and we restricted the analyses to those relevant to utility locating near the surface of the earth. Future studies may choose a different range of values that are suited to other particular areas of interest. Beside frequency, other electromagnetic properties are also of interest. We are currently investigating the effect of permeability (magnetic soils) on utility locating, as well as an analytical model that is capable of treating a wire located near a dielectric half-space (above, at, or below the interface).

The contributions of this work are many. A broad set of parameters (relevant to locating buried linear conductors) has been chosen as inputs into the simulations, which has shed light on the electromagnetic scattering. This was enabled by the fact that we have implemented a numerical solver to calculate the current distribution, thereby avoiding any restrictions or assumptions that often accompany analytical methods. Moreover, the current excitation process has been studied under three environmental conditions: free-space, full-space, and half-space. Each of these has relevant sensing applications. We also consider the excitation using various electromagnetic sources, again, with a view towards generality and the ability to compare results between the different excitation modalities. Indeed, the results presented herein, as well as those of future studies, will assist in further understanding electromagnetic scattering from linear conductors and aid in the optimization of devices used to detect them.

References

[1] S. E. Irvine. Experimental measurements of the response of a single-transmitter receiver electromagnetic induction sensor to a linear conductor. IEEE Geosci. Remote S., 9:462–466, 2012.

[2] K. Tsubota and J. R. Wait. The frequency and the time-domain responses of a buried axial conductor. Geophysics, 45:941–951, 1980.

[3] D. A. Hill. Magnetic dipole excitation of an insulated conductor of finite length. IEEE T. Geosci. Remote., 28:289–294, 1990.

[4] D. A. Hill. Magnetic Dipole Excitation of a Long Conductor in a Lossy Medium. IEEE T. Geosci. Remote., 26:720–725, 1988.

[5] R.W.P. King, P. F. Sforza, and T.I.S. Boak III, The current in a parasitic antenna in a dissipative medium. IEEE T. Antenn. Propag., 22:809– 814, 1974.

[6] R. P. W. King. The insulated conductor as a scattering antenna in a relatively dense medium. IEEE T. Antenn. Propag., 24(3):327–330, 1976.

[7] R.W.P. King and L. C. Shen. Scattering by wires by a material half- space. IEEE T. Antenn. Propag., 30:1165–1171, 1982.

[8] R. G. Olsen and M. Utsa. The excitation of current on an infi horizontal wire above earth by a vertical electric dipole. IEEE T. Antenn. Propag., 25:560–565, 1977.

[9] R.G. Olsen and D. Chang. Current induced by a plane wave on a thin infinite wire near the earth. IEEE T. Antenn. Propag., 22:586–589, 1974.

[10] R. G. Olsen and A. Aburwein. Current induced on a pair of wires above earth by a vertical electric dipole for grazing angles of incidence. Radio Science, 15:733–742, 1980.

[11] D. Poljak, F. Rachidi, and S.V. Tkachenko. Generalized form of telegrapher's equations for the electromagnetic field coupling to finite-length lines above a lossy ground. IEEE T. Electromagn. C., 49(3):689–697, 2007.

[12] D. Poljak, V. Doric, F. Rachidi, K. Drissi, K. Kerroum, S.V. Tkachenko, and S. Sesnic. Generalized form of telegrapher's equations for the electromagnetic field coupling to buried wires of finite length. IEEE T. Electromagn. C., 51(2):331–337, 2009.

[13] H. W. L. Naus. Modeling of buried wire detection by radio-frequency electromagnetic waves. IEEE Geosci. Remote S., 10(1):160–164, 2013.

[14] S. E. Irvine. Numerical simulation of wire detection using radio-frequency transmitter-receiver pairs. DRDC Suffield Technical Memorandum 2010-041, DRDC Suffield, 2010.

[15] B. Rembold, H. G. Wippich, M. Bischoff and W. F. X. Frank. A mm-wave collision warning sensor for helicopters. Proc. Military Microwave, pages 344–351, 1982.

[16] H. Essen, S. Boehmsdorff, G. Biegel, and A. Wahlen. On the scattering mechanism of power lines at millimeter-waves. IEEE T. Geosci. Remote., 40:1895–1903, 2002.

[17] A. Kumar. RCS measurements detect power lines. Microwaves & RF, 43:82, 2004.

[18] K. Sarabandi and M. S. Park. Millimeter-wave radar phenomenology of power lines and a polarimetric detection algorithm. IEEE T. Antenn. Propag., 47:1807–1813, 1999.

[19] K. E. Potter. Techniques for Overhead-Wire Detection. IEE Proc. F, 128:427–432, 1981.

[20] R. Appleby, P. Coward, and J. N. Sanders-Reed. Evaluation of a passive millimeter-wave (pmmw) imager for wire detection in degraded visual conditions. In R. Appleby and D. A. Wikner, editors, Passive Millimeter-Wave Imaging Technology XII, volume 7309, pages 1–8. Proc. SPIE, 2009.

[21] S. Ebihara and Y. Hashimoto. MOM analysis of dipole antennas in cross-hole borehole radar and fi experiments. IEEE T. Geosci. Remote, 45(8):2435–2450, 2007.

[22] N. Metje, P. R. Atkins, M. J. Brennan, D. N. Chapman, H. M. Lim, J. Machell, J. M. Muggleton, S. Pennock, J. Ratcliffe, M. Redfern, C. D. F. Rogers, A. J. Saul, Q. Shan, S. Swingler, and A. M. Thomas. Mapping the underworld–State-of-the-art review. Tunn. Undergr. Sp. Tech., 22:568–586, 2007.

[23] B. T. Kolera and L. E. Bernold. Intelligent utility locating tool for excavators. J. Constr. Eng. M. ASCE, 132:919–927, 2006.

[24] R. F. Harrington. Field Computation by Moment Methods. Robert E. Krieger Publishing Company, Inc., 1968.

[25] U. Jakobus. Comparison of different techniques for the treatment of lossy dielectric/magnetic bodies within the method of moments formulation. AEU Int. J. Electron. Commun., 54:163–173, 2000.

[26] S. Ramo, J. R. Whinnery, and T. Van Duzer. Fields and Waves in Communications Electronics. Wiley, 3rd edition, 1994.

[27] R.W.P. King, G.J. Fikioris and R.B. Mack, Cylindrical Antennas and Arrays, Cambridge University Press, New York.

[28] J. R. Gray. Conductivity analyzers and their application. In R. D. Down and J. H. Lehr, editors, Environmental Instrumentation and Analysis Handbook, pages 491–510. Wiley, 2004.

[29] M. N. Hill (ed.). The Sea, volume 1. Interscience, 1962.

[30] M. N. Hill (ed.). The Sea, volume 4, pt 1, chap. 18. Wiley, 1971.

[31] R. A. Cox, M. J. McCartney, and F. Culkin. The specific gravity/salinity/temperature relationship in natural sea water: Deep Sea Res., 17:679–689, 1970.

[32] W. C. Gibson. The Method of Moments in Electromagnetics. Chapman and Hall, 2007.

[33] D. Campbell, private communication.

[34] J. K. E. Tunaley and S. E. Irvine, unpublished.

This page intentionally left blank.

Annex A Comparison with Analytical Model

In order to provide confidence in the model results presented here, additional comparisons with a recently developed analytical model [34] are presented. This analytical model is based on a transmission line (TL) approach and is capable of treating wires located at a dielectric half-space. The wire parameters used for the comparison are identical to those described above in Section 2. The soil permittivity is fixed at $\varepsilon_e = 2.5\varepsilon_0$, while frequency and soil conductivity are varied. Figure A.1 illustrates several current distributions, as predicted by FEKO and the half-space model, in a free-space environment. Good agreement is observed, even despite using a transmission line approach (which would have no physical return path in free space). Figures A.2 and A.3 illustrate similar comparisons for the full and half-spaces, respectively. In these cases, excellent agreement is achieved. It is noted that, at the time of publication of this report, the half-space transmission line model is undergoing further development and refinement. A complete analysis and description of the model will form the basis of a future manuscript.

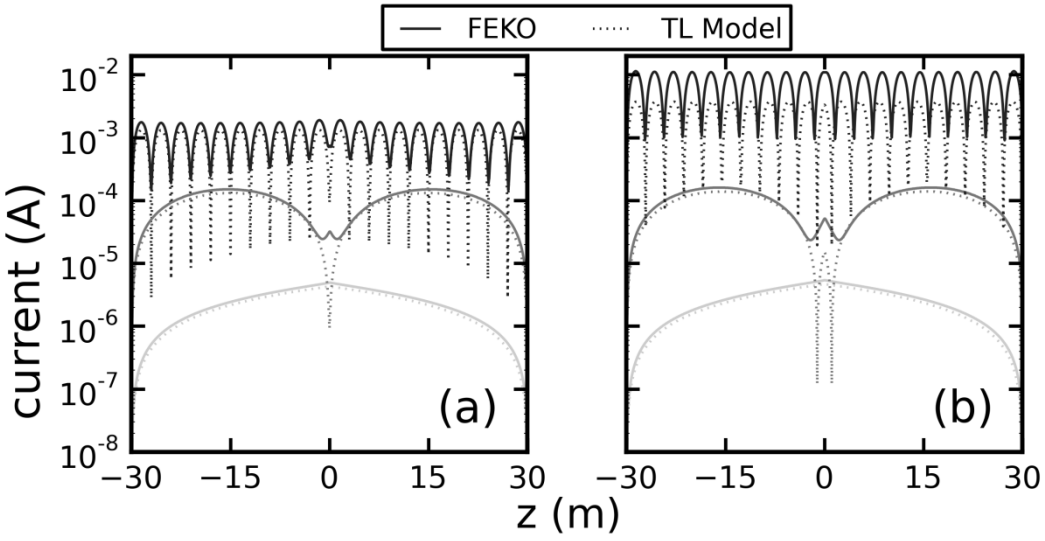

Figure A.1: *Comparison of current distributions generated in a wire in free-space, as predicted by FEKO and a recently developed analytical transmission line model (presently under development. Frequencies chosen for comparison were f=500 kHz, 5 MHz, and 50 MHz for both bare (a) and insulated (b) wire.*

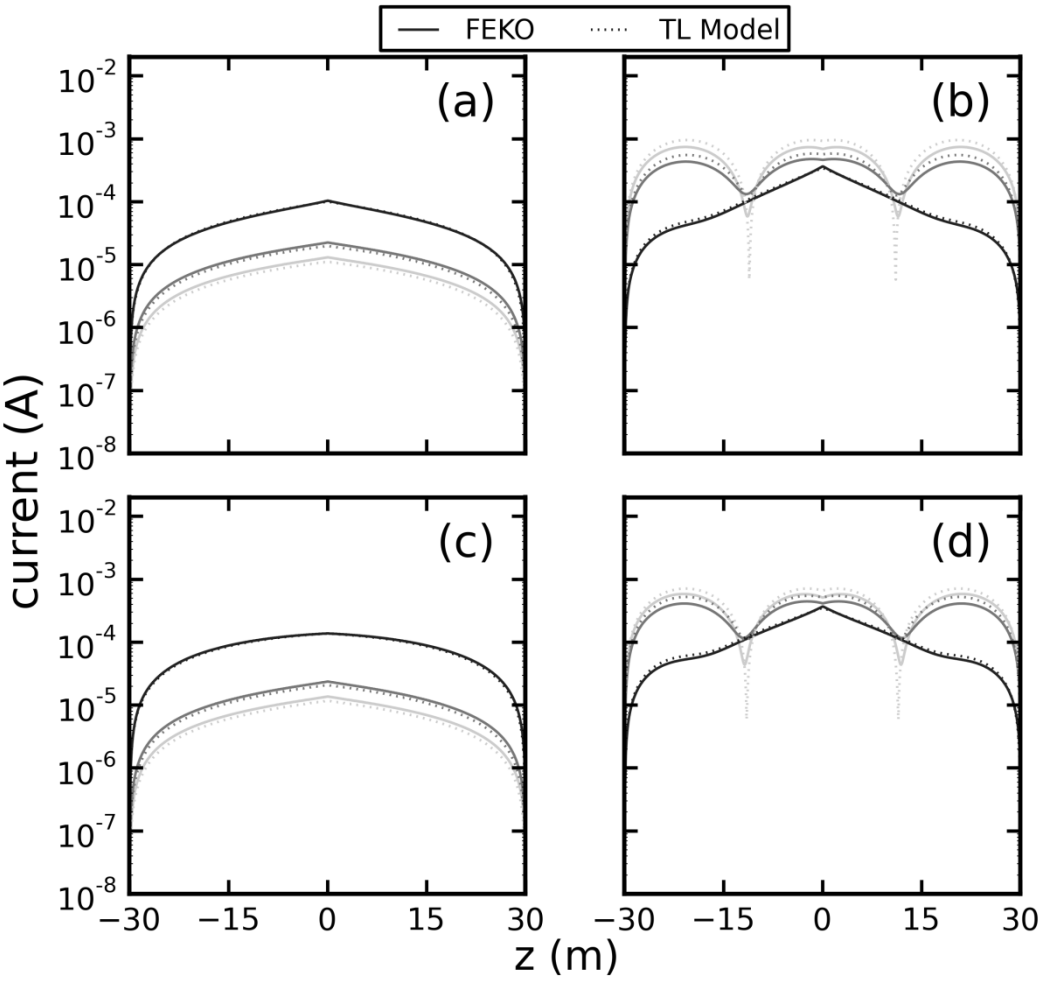

Figure A.2: *Comparison of current distributions generated in a wire in a full-space environment, as predicted by FEKO and a recently developed analytical transmission line model (presently under development). The relative permittivity of the ground is held at 2.5 while σ_e takes on values 0 (light grey), 1×10^{-4} S/m (gray), and 1×10^{-3} S/m (black). Analysis was performed for various combinations of frequency and wire coating, which are (a) bare and 500 kHz, (b) bare and 5 MHz, (c) insulated and 500 kHz, and (d) insulated and 5 MHz.*

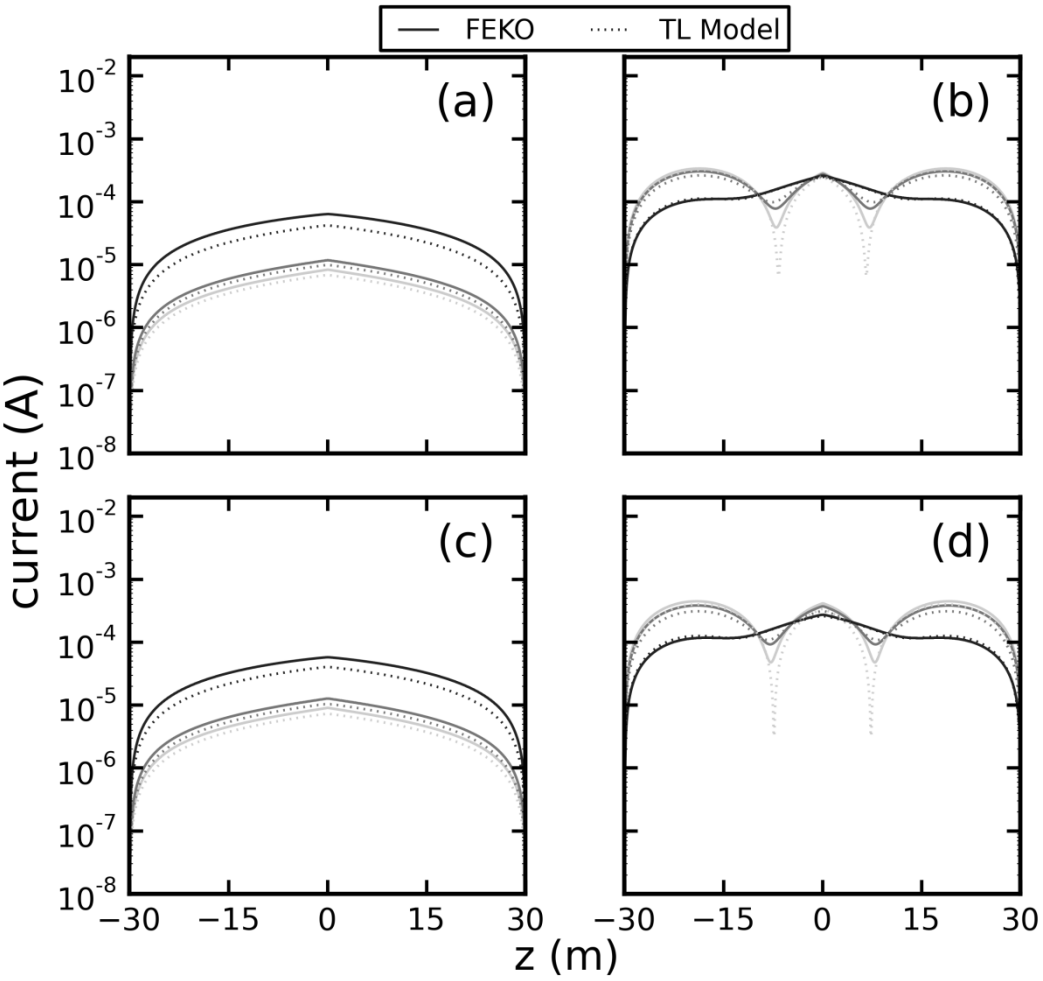

Figure A.3: *Comparison of current distributions generated in a wire in a half-space environment, as predicted by FEKO and a recently developed analytical transmission line model (presently under development). The relative permittivity of the ground is held at 2.5 while* σ_e *takes on values 0 (light grey),* 1×10^{-4} *S/m (gray), and* 1×10^{-3} *S/m (black). Analysis was performed for various combinations of frequency and wire coating, which are (a) bare and 500 kHz, (b) bare and 5 MHz, (c) insulated and 500 kHz, and (d) insulated and 5 MHz.*

This page intentionally left blank.

DOCUMENT CONTROL DATA

(Security markings for the title, abstract and indexing annotation must be entered when the document is Classified or Designated)

1. ORIGINATOR (The name and address of the organization preparing the document. Organizations for whom the document was prepared, e.g., Centre sponsoring a contractor's report, or tasking agency, are entered in Section 8.)

DRDC – Suffield Research Centre
Defence Research and Development Canada
P.O. Box 4000, Station Main
Medicine Hat, Alberta T1A 8K6
Canada

2a. SECURITY MARKING (Overall security marking of the document including special supplemental markings if applicable.)

UNCLASSIFIED

2b. CONTROLLED GOODS

(NON-CONTROLLED GOODS)
DMC A
REVIEW: GCEC APRIL 2011

3. TITLE (The complete document title as indicated on the title page. Its classification should be indicated by the appropriate abbreviation (S, C or U) in parentheses after the title.)

Parametric Modeling of the Current Induced in Linear Conductors

4. AUTHORS (last name, followed by initials – ranks, titles, etc., not to be used)

Sooriyadevan, P.; Tunaley, J.; Irvine, S. E.

5. DATE OF PUBLICATION (Month and year of publication of document.)	6a. NO. OF PAGES (Total containing information, including Annexes, Appendices, etc.)	6b. NO. OF REFS (Total cited in document.)
July 2015	34	34

7. DESCRIPTIVE NOTES (The category of the document, e.g., technical report, technical note or memorandum. If appropriate, enter the type of report, e.g., interim, progress, summary, annual or final. Give the inclusive dates when a specific reporting period is covered.)

Scientific Report

8. SPONSORING ACTIVITY (The name of the department project office or laboratory sponsoring the research and development – include address.)

DRDC – Suffield Research Centre
Defence Research and Development Canada
P.O. Box 4000, Station Main
Medicine Hat, Alberta T1A 8K6
Canada

9a. PROJECT OR GRANT NO. (If appropriate, the applicable research and development project or grant number under which the document was written. Please specify whether project or grant.)	9b. CONTRACT NO. (If appropriate, the applicable number under which the document was written.)

10a. ORIGINATOR'S DOCUMENT NUMBER (The official document number by which the document is identified by the originating activity. This number must be unique to this document.)	10b. OTHER DOCUMENT NO(s). (Any other numbers which may be assigned this document either by the originator or by the sponsor.)
DRDC-RDDC-2015-R108	

11. DOCUMENT AVAILABILITY (Any limitations on further dissemination of the document, other than those imposed by security classification.)

Unlimited

12. DOCUMENT ANNOUNCEMENT (Any limitation to the bibliographic announcement of this document. This will normally correspond to the Document Availability (11). However, where further distribution (beyond the audience specified in (11) is possible, a wider announcement audience may be selected.))

Unlimited

13. ABSTRACT (A brief and factual summary of the document. It may also appear elsewhere in the body of the document itself. It is highly desirable that the abstract of classified documents be unclassified. Each paragraph of the abstract shall begin with an indication of the security classification of the information in the paragraph (unless the document itself is unclassified) represented as (S), (C), (R), or (U). It is not necessary to include here abstracts in both official languages unless the text is bilingual.)

This report presents computational results of the amplitude of the induced current in a linear conductor and the variation of the amplitude under different external excitation and electromagnetic conditions. For location and avoidance of buried utility cables, the ability to detect linear conductors with a high degree of confidence is important. The report begins with a brief survey of modeling of current induction in conductors and a description of the geometry of the problem, followed by a parametric model analysis using a commercially-available Method-of-Moments solver. The variables addressed in this work are frequency of excitation (50 kHz to 50 MHz), excitation source (plane-wave or dipole), and conductor radius, as well as the conductivity and permittivity of the surrounding soil. The findings herein, as well as those of follow-on studies, will assist in the understanding of electromagnetic scattering from linear conductors and aid in the optimization of devices used to locate them.

Ce rapport présente les résultats computationnels liés à l'amplitude du courant induit dans un conducteur linéaire et à l'écart en amplitude dans des conditions électromagnétiques et d'excitation externe différentes. Pour pouvoir repérer et éviter les câbles enfouis des services publics, il importe d'avoir la capacité de détecter avec très grande certitude les conducteurs linéaires. Le rapport débute par un bref survol de la modélisation de courant induit dans des conducteurs et une description de la géométrie du problème, puis par l'analyse d'un modèle paramétrique au moyen d'un solveur commercial faisant appel à la méthode des moments. Dans ces travaux, on examine les variables suivantes : fréquence de l'excitation (50 kHz à 50 MHz); source de l'excitation (onde plane ou dipôle); rayon des conducteurs; conductivité et permittivité du sol environnant. Les conclusions fournies dans le rapport et celles tirées d'études de suivi aideront à comprendre la diffusion électromagnétique des conducteurs linéaires tout en contribuant à l'optimisation des appareils utilisés pour repérer ceux-ci.

14. KEYWORDS, DESCRIPTORS or IDENTIFIERS (Technically meaningful terms or short phrases that characterize a document and could be helpful in cataloguing the document. They should be selected so that no security classification is required. Identifiers, such as equipment model designation, trade name, military project code name, geographic location may also be included. If possible keywords should be selected from a published thesaurus, e.g., Thesaurus of Engineering and Scientific Terms (TEST) and that thesaurus identified. If it is not possible to select indexing terms which are Unclassified, the classification of each should be indicated as with the title.)

Wire Scattering, Electromagnetic Scattering, Induction